Formation of [CH4-Fe]q (q = -1, 0, +1) complexes and oxidative addition of methane to Feq atoms. A qualitative molecular orbital study

Eloy N. Rodriguez-Arias, Luis Rincon, and Fernando Ruette

More About This Article

The permalink http://dx.doi.org/10.1021/om00059a034 provides access to:

- Links to articles and content related to this article
- Copyright permission to reproduce figures and/or text from this article

Formation of $[CH_4-Fe]^q$ ($q = -1, 0, +1$) Complexes and Oxidative Addition of Methane to Fe^q Atoms. A Qualitative Molecular Orbital Study

Eloy N. Rodríguez-Arias,[†,‡] Luis Rincón,[†] and Fernando Ruette*,[§]

Departamento de Química, Universidad Simón Bolívar, Apartado 89000, Caracas 1080-A, Venezuela, and Centro de Química, Laboratorio de Química Computacional, Instituto Venezolano de Investigaciones Científicas, IVIC, Apartado 21827, Caracas 1020-A, Venezuela

The formation of $[CH_4-Fe]^q$ complexes and the oxidative addition of methane to iron metal centers Fe^q ($q = +1, 0, -1$) was studied by using the MINDO/SR-UHF method. The methane-Fe interaction was examined by optimizing several geometries with C_{3v}, C_{2v}, and C_s symmetries. Diatomic energies, bond orders, and electronic configuration of metallic centers have been correlated with the interaction energy among the components of the system. The potential energy curves for the oxidative addition of the intermediate species were calculated for C_s symmetry. Results show that the formation of intermediates and the oxidative addition are favored as the system between negatively charged, suggesting that an electronic transfer from the metal to the methane promotes the C-H bond activation. It was also found that an increase in the p character of the metal center favors the C-H bond-dissociation process.

Introduction

Methane is the major component of natural gas and is primarily used as a fuel.[1] The abundance of methane makes it a raw material of the greatest synthetic importance. The profitable conversion of methane to useful chemicals has increased recently;[2,3] therefore alkane activation is a topic of great interest in organometallic chemistry and catalysis research. It is possible to distinguish three types of C-H bond activation in alkanes by metals:[1b]

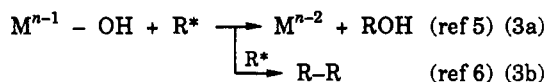(a) Activation on reduced metals that leads to an oxidative addition:

$$M^n + R{-}H \rightarrow M^{n+2}RH \qquad (1)$$
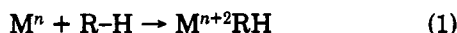
For example, the photoactivation of organometallic complexes:
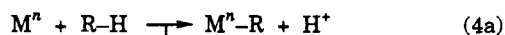
$$LL'MH_2 \xrightarrow[-H_2]{h\nu} LL'M \xrightarrow{+RH} LL'MRH \qquad (2)$$
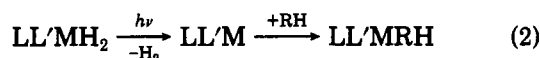
where $L = \eta^5\text{-}C_5Me_5$, $L' = PMe_3$, and $M = Rh$, Ir.[4]

(b) Activation on metal oxides through free radicals:[5,6]

$$M^n = O + R{-}H \rightarrow$$

$$M^{n-1} - OH + R^* \longrightarrow M^{n-2} + ROH \quad (\text{ref }5) \quad (3a)$$
$$\phantom{M^{n-1} - OH + R^*} \xrightarrow{R^*} R{-}R \quad (\text{ref }6) \quad (3b)$$

For example, methane activation on Li/MgO[6b] and oxides of Sn, Pb, Sb, Bi, Tl, Cd, and Mn.[6a]

(c) Electrophilic activation:[7]

$$M^n + R{-}H \longrightarrow M^n{-}R + H^+ \quad (4a)$$
$$\phantom{M^n + R{-}H} \longrightarrow M^n{-}H + R^+ \quad (4b)$$

For example, $Pt(II) + CH_4 \rightarrow Pt^{II}CH_3 + H^+$.[7b]

The interactions of saturated hydrocarbons with metallic centers in organometallic complexes, bare and ligated metal ions, and metal fragments have received attention by theoretical and experimental chemists.[8-12] However, the analysis of energetic and electronic factors that influence the formation of metal-H and metal-C bonds and the

scission of the C-H bonds in metallic centers has not been completed. Modifications of the electronic distribution

(1) (a) Saint-Just, J.; Garat, A. Rev. Energ. 1986, 285, 2. (b) Mimoun, H. New. J. Chem. 1987, 11, 513.
(2) (a) Chang, C. D.; Silvestri, A. J. J. Catal. 1977, 47, 249. (b) Gesser, H. D.; Hunter, N. R. Chem. Rev. 1985, 85, 235. (c) Anderson, J. R. Appl. Catal. 1989, 47, 177.
(3) (a) Crabtree, R. H. Chem. Rev. 1985, 85, 245. (b) Green, M. L. H.; O'Hare, D. Pure. Appl. Chem. 1985, 57, 1897. (c) Jones, W. D.; Feher, F. J. J. Am. Chem. Soc. 1985, 107, 620. (d) Halpern, J. Inorg. Chim. Acta 1985, 100, 41. (e) Ephritikhine, M. Nouv. J. Chim. 1986, 10, 9. (f) Crabtree, R. H.; Hamilton, D. G. Adv. Organomet. Chem. 1988, 28, 299. (g) Brown, S. H.; Crabtree, R. H. J. Am. Chem. Soc. 1989, 111, 2935. (h) Crabtree, R. H. Acc. Chem. Res. 1990, 23, 95.
(4) Janowicz, A. H.; Periana, R. A.; Buchanan, J. M.; Kovac, C. A.; Stryker, J. M.; Wax, M. J.; Bergman, R. G. Pure. Appl. Chem. 1984, 56, 13 and references therein.
(5) Wiberg, K. B. In Oxidation in Organic Chemistry; Academic Press: New York, 1965; Part A, p 69.
(6) (a) Keller, G. E.; Bhasin, M. M. J. Catal. 1982, 73, 9. (b) Driscoll, D. J.; Martir, W.; Wang, J.-X.; Lundsford, J. H. J. Am. Chem. Soc. 1985, 107, 58. (c) Pitchai, R.; Klier, H. Catal. Rev.-Sci. Eng. 1986, 28, 14. (d) Labinger, J. A.; Ott, K. C. J. Phys. Chem. 1987, 91, 2682. (e) Lee, J. S.; Oyama, S. T. Catal. Rev.-Sci. Eng. 1988, 30, 249. (f) Hutchings, G. J.; Scurrell, M. S.; Woodhouse, J. R. Chem. Soc. Rev. 1989, 18, 251.
(7) (a) Bruno, J. W.; Marks, T. J.; Day, V. W. J. Am. Chem. Soc. 1982, 104, 7357. (b) Kusch, L. A.; Lavrushko, V. V.; Misharin, Y. S.; Moravsky, A. P.; Shilov, A. E. Nouv. J. Chim. 1983, 7, 729. (c) Watson, P. L. J. Am. Chem. Soc. 1983, 105, 6491. (d) Kitajima, K.; Schwartz, J. J. Am. Chem. Soc. 1984, 106, 2220. (e) Teuben, J. H. Fundamental and Technological Aspects of Organo-f-Element Chemistry; Marks, T. J., Fragala, I. L., Eds.; NATO ASI Series, D. Reidel: Boston, 1985; p 195. (f) Fendrick, C. M.; Marks, T. J. J. Am. Chem. Soc. 1986, 108, 425. (g) Thompson, M. E.; Baxter, S. M.; Bulls, A. R.; Burger, B. J.; Nolan, M. C.; Santarsiero, B. D.; Schaefer, W. P.; Bercaw, J. E. J. Am. Chem. Soc. 1987, 109, 203 and references therein.
(8) (a) Baetzold, R. C. J. Am. Chem. Soc. 1983, 105, 4271. 9b) Shustorovich, E.; Baetzold, B. C.; Muetterties, E. L. J. Phys. Chem. 1983, 87, 1100.
(9) Saillard, J.-Y.; Hoffmann, R. J. Am. Chem. Soc. 1984, 106, 2006.
(10) (a) Gavin, R. M., Jr.; Reutt, J.; Muetterties, E. L. Proc. Natl. Acad. Sci. U.S.A. 1981, 78, 3981. (b) Muetterties, E. L. Chem. Soc. Rev. 1982, 11, 283. (c) Minot, C.; Van Hove, M. A.; Somorjai, G. A. Surf. Sci. 1983, 127, 441. (d) Blomberg, M. R. A.; Brandemark, U.; Petterson, L.; Siegbahn, P. E. M. Int. J. Quantum Chem. 1983, 23, 855. (f) Blomberg, M. R. A.; Brandemark, U.; Siegbahn, P. E. M. J. Am. Chem. Soc. 1983, 105, 5557. (g) Siegbahn, P. E. M.; Blomberg, M. R. A.; Bauschlicher, C. W., Jr. J. Chem. Phys. 1984, 81, 1373. (h) Brandemark, U. B.; Blomberg, M. R. A.; Petterson, L. G. M.; Siegbahn, P. E. M. J. Phys. Chem. 1984, 88, 4617. (i) Eller, K.; Schwarz, H. Chem. Rev. 1991, 91, 1121.
(11) (a) Low, J. J.; Goddard III, W. A. J. Am. Chem. Soc. 1984, 106, 6928. (b) Low, J. J.; Goddard III, W. A. J. Am. Chem. Soc. 1984, 106, 8321. (c) Low, J. J.; Goddard III, W. A. Organometallics 1986, 5, 609. (d) Particularly, Low and Goddard verified that the electronic state has a marked influence in the dihydrogen activation reaction on the palladium and platinum centers. They observed an activation barrier diminution when there is an electronic state change on the metallic center from d^8s^2 to d^9s^1 to d^{10}. Low, J. J.; Goddard III, W. A. J. Am. Chem. Soc. 1986, 108, 6115.

†Universidad Simón Bolívar.
‡Visiting Fellow, Centro de Química, Laboratorio de Química Computacional, IVIC, Apartado 21827, Caracas 1020-A, Venezuela.
§Instituto Venezolano de Investigaciones Cientificas.

Table I. Bonding and Electronic Properties of [FeCH$_4$]^q with $q = 0$ in C_{3v}, C_{2v}, and C_s Symmetries^a

property	Fe–H^1	Fe–C	C–H^1	C–H^2	Fe	C	H^1
Symmetry C_{3v}, EC(Fe) = s$^{0.92}$p$^{0.41}$d$^{6.99}$; IE = –8.4 kcal/mol							
EBD (Å)	2.192	2.131	1.134	1.120			
MBO	0.25	0.81	1.13	1.19			
DE (au)	–0.038	–0.269	–0.394	–0.433			
charge (au)					–0.32	+0.15	+0.09
Symmetry C_{2v}, EC(Fe) = s$^{0.93}$p$^{0.38}$d$^{6.99}$, IE = –3.4 kcal/mol							
EBD (Å)	2.035	2.236	1.134	1.118			
MBO	0.34	0.71	1.12	1.21			
DE (au)	–0.055	–0.230	–0.383	–0.433			
charge (au)					–0.30	+0.14	+0.13
Symmetry C_s, EC(Fe) = s$^{0.98}$p$^{0.14}$d$^{7.00}$, IE = –5.5 kcal/mol							
EBD (Å)	2.074	2.792	1.101	1.107			
MBO	0.31	0.29	1.18	1.23			
DE (au)	–0.041	–0.071	–0.408	–0.441			
charge (au)					–0.12	+0.07	+0.09

^{a} H^1 and H^2 are hydrogen atoms shown in Figure 1.

on a modeled center site can be carried out by altering its electronic environment (ligands), modifying the electronic charge, and changing its electronic state.[13] Several calculations have been performed by using one single metal atom as model of adsorption site, for example H$_2$ on Ni[14] and [Fe]^q (q = –1, 0, +1),[15] O$_2$ on [Fe]^q (q = –1, 0, +1, +2),[16] [Co]^q (q = –1, 0, +1, +2, +3),[17] and [Ni]^q (q = 0, +2),[18] and N$_2$ on a [Fe]^q (q = –1, 0, +1).[19]

The purpose of the present study is to evaluate thermodynamic (energy changes between reactants and products), electronic (effect of electronic charge on active site), and kinetic factors (energy barriers) that affect the oxidative addition of methane on one iron atom, in different oxidation states. In this work, one iron atom has been used as a model of a catalytic center for studying the methane activation, based on three reasons:

(i) A single iron atom can activate methane C–H bonds, as has been established by experiments of Billups et al.,[13a] Margrave and Kafafi,[13b] Ozin et al.,[13d,e] and Armentrout and Beauchamp.[13g]

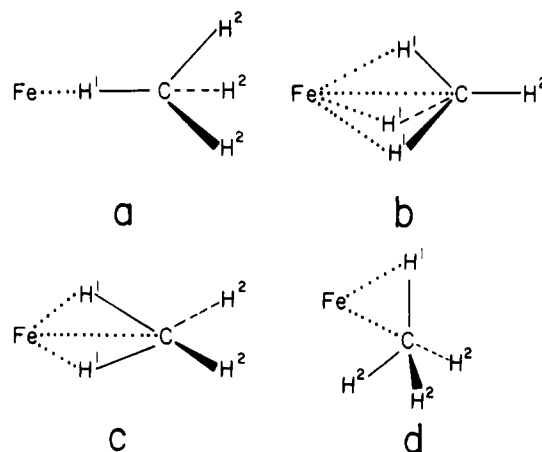(ii) As pointed out above, an iron atom has been used as a model of one-center active site on catalytic reactions.

(12) Ziegler, T.; Tschinke, V.; Fan, L.; Becke, A. D. *J. Am. Chem. Soc.* **1989**, *111*, 9177.

(13) (a) Billups, W. E.; Konarski, M. M.; Hauge, R. H.; Margrave, J. L. *J. Am. Chem. Soc.* **1980**, *102*, 7393. (b) Kafafi, Z. H.; Hauge, R. H.; Margrave, J. L. *J. Am. Chem. Soc.* **1985**, *107*, 6134 and references therein. (c) Chang, S.-C.; Hauge, R. H.; Margrave, J. L.; Billups, W. E. *J. Am. Chem. Soc.* **1988**, *110*, 7975. (d) Ozin, G. A.; McCaffrey, J. G.; McIntosh, D. F. *Pure Appl. Chem.* **1984**, *56*, 111. (e) Ozin, G. A.; McCaffrey, J. G.; Parnis, J. M. *Angew. Chem., Int. Ed. Engl.* **1986**, *25*, 1072 and references therein. (f) Murray, V.; Field, L. *J. Am. Chem. Soc.* **1987**, *109*, 2825. (g) Armentrout, P. B.; Beauchamp, J. L. *Acc. Chem. Res.* **1989**, *22*, 315. (h) Martinho Simoes, J. A.; Beauchamp, J. L. *Chem. Rev.* **1990**, *90*, 629. (i) Eller, K.; Schwarz, H. *Chem. Rev.* **1991**, *91*, 1121. (j) Harper, T. G. P.; Shinomoto, R. S.; Deming, M. A.; Flood, T. C. *J. Am. Chem. Soc.* **1988**, *110*, 7915. (k) Bullock, R. M.; Headford, C. E. L.; Hennessy, K. M.; Kegley, S. E.; Norton, J. R. *J. Am. Chem. Soc.* **1989**, *111*, 3897. (l) Shinomoto, R. S.; Desrosiers, P. J.; Harper, T. G. P.; Flood, T. C. *J. Am. Chem. Soc.* **1990**, *112*, 704. (m) Brookhart, M.; Green, M. L. H. *J. Organomet. Chem.* **1983**, *250*, 395. (n) Brookhart, M.; Green, M. L. H.; Wong, L.-L. *Prog. Inorg. Chem.* **1988**, *36*, 1. (o) Perutz, R. N.; Belt, S. T.; McCamley, A. Whittlesey, M. K. *Pure Appl. Chem.* **1990**, *62*, 1539. (p) Barret, P. H.; Pasternak, M.; Pearson, R. G. *J. Am. Chem. Soc.* **1979**, *101*, 222. (q) Field, L. D.; George, A. V.; Messerle, B. A. *J. Chem. Soc., Chem. Commun.* **1991**, 1339.

(14) Ruette, F.; Blyholder, G.; Head, J. *J. Chem. Phys.* **1984**, *80*, 2042.

(15) Sánchez, M.; Ruette, F.; Hernández, A. J. *J. Phys. Chem.* **1992**, *96*, 823.

(16) Blyholder, G.; Head, J.; Ruette, F. *Inorg. Chem.* **1982**, *21*, 1539.

(17) Hernández, A. J.; Ruette, F.; Ludeña, E. V. *J. Mol. Catal.* **1987**, *39*, 21.

(18) Castejón, H.; Hernández, A. J.; Ruette, F. *J. Phys. Chem.* **1988**, *92*, 4970.

(19) Rincón, L.; Ruette, F.; Hernández, A. J. *J. Mol. Struct. (THEOCHEM)* **1991**, *254*, 395.

Figure 1. Geometries of FeCH$_4$ intermediates: (a) C_{3v}; (b) C_{3v}; (c) C_{2v}; (d) C_s symmetries.

(iii) There are organometallic complexes (monometallic) that activate the methane C–H bond.[4,13f-m,q]

The method used was MINDO/SR-UHF (MINDO/3 adapted for transition metals). Methane activation was studied starting from several interaction geometries and different electronic charges on the active site, in order to examine, as a first step, the formation of Fe–CH$_4$ intermediates (a model of adsorbed species). Potential energy curves for the C_s symmetry were calculated by optimizing bond distances at different Fe–C–H angles, in order to study, as second step, the dissociation of a C–H bond (see eq 5, where q = +1, 0, –1).

$$\text{Fe}^q + \text{CH}_4 \rightarrow [\text{Fe–CH}_4]^q \rightarrow [\text{H–Fe–CH}_3]^q \qquad (5)$$
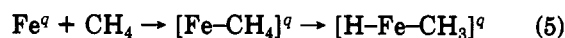
Theoretical Method

The semiempirical method MINDO/SR used in this study[20] is an adaptation of MINDO/3[21] for transition metals, based on the algorithm described by Rinaldi.[22] The modification of MINDO/3 also includes the computation of symmetry-adapted wave functions and selective occupation of molecular orbital functions. These characteristics are very useful for calculating potential energy surfaces, since they allow one to maintain fixed electronic states along the reaction coordinate. The monoatomic and

(20) Blyholder, G.; Head, J.; Ruette, F. *Theor. Chim. Acta* **1982**, *60*, 429.

(21) Bingham, R.; Dewar, M. J. S.; Lo, D. H. *J. Am. Chem. Soc.* **1975**, *97*, 1285.

(22) Rinaldi, D. *Comput. Chem.* **1976**, *1*, 109.

Table II. Bonding and Electronic Properties of $[FeCH_4]^q$ with $q = +1$ in C_{3v}, C_{2v}, and C_s Symmetries[a]

property	Fe-H¹	Fe-C	C-H¹	C-H²	Fe	C	H¹
Symmetry C_{3v}, EC(Fe) = $s^{0.18}p^{0.37}d^{7.00}$; IE = −49.56 kcal/mol							
EBD (Å)	2.099	2.010	1.156	1.114			
MBO	0.34	1.05	1.06	1.22			
DE (au)	−0.037	−0.348	−0.367	−0.435			
charge (au)					+0.45	+0.048	+0.15
Symmetry C_{2v}, EC(Fe) = $s^{0.19}p^{0.33}d^{7.00}$, IE = −42.95 kcal/mol							
EBD (Å)	1.942	2.093	1.166	1.118			
MBO	0.45	0.96	1.02	1.21			
DE (au)	−0.054	−0.315	−0.347	−0.430			
charge (au)					+0.48	+0.06	+0.17
Symmetry C_s, EC(Fe) = $s^{0.14}p^{0.18}d^{7.00}$, IE = −19.56 kcal/mol							
EBD (Å)	1.795	2.612	1.112	1.167			
MBO	0.58	0.48	1.06	1.23			
DE (au)	−0.088	−0.122	−0.341	−0.446			
charge (au)					+0.68	+0.10	+0.06

[a] H¹ and H² are hydrogen atoms shown in Figure 1.

Table III. Bonding and Electronic Properties of $[FeCH_4]^q$ with $q = -1$ in C_{3v}, C_{2v}, and C_s Symmetries[a]

property	Fe-H¹	Fe-C	C-H¹	C-H²	Fe	C	H¹
Symmetry C_{3v}, EC(Fe) = $s^{0.89}p^{0.68}d^{6.99}$, IE = −94.85 kcal/mol							
EBD (Å)	2.325	1.941	1.221	1.205			
MBO	0.18	1.22	0.82	1.05			
DE (au)	−0.007	−0.538	−0.298	−0.405			
charge (au)					−0.56	+0.40	−0.20
Symmetry C_{2v}, EC(Fe) = $s^{0.29}p^{1.15}d^{6.96}$; IE = −72.39 kcal/mol							
EBD (Å)	2.084	1.806	1.314	1.205			
MBO	0.32	1.61	0.59	0.91			
DE (au)	−0.027	−0.727	−0.209	−0.351			
charge (au)					−0.42	+0.35	−0.16
Symmetry C_s, EC(Fe) = $s^{0.96}p^{0.27}d^{7.00}$; IE = −48.69 kcal/mol							
EBD (Å)	1.922	2.737	1.212	1.171			
MBO	0.48	0.37	0.98	0.95			
DE (au)	−0.070	−0.111	−0.294	−0.351			
charge (au)					−0.23	+0.20	−0.06

[a] H¹ and H² are hydrogen atoms shown in Figure 1.

diatomic parameters used in this paper have been taken from ref 23 except the Fe–C parameters, which were selected from Lawless and Blyholder's work.[24] With these parameters, the reference state of the Fe atom was $^5F(s^1d^7)$. This represents a more realistic model of a one-center site on an iron surface, since in previous calculations with iron clusters the surface atoms present more or less a s^1d^7 electronic configuration.[19,23]

The theoretical results in this paper will be discussed on the basis of bond orders, diatomic energies, equilibrium bond distances, electronic charge densities, interaction energies, molecular orbital diagrams, and potential energy curves. Due to the fact that a search for the most stable electronic states and an exhaustive parametrization were not performed, these results presented here are essentially qualitative.

C–H Bond Activation

The geometrical structures of Fe–CH₄, shown in Figure 1, were chosen as interaction models to study the methane bonding with a metallic center modeled by Fe^q ($q = +1$, 0, −1). The geometries a–d correspond to C_{3v}, C_{3v}, C_{2v}, and C_s symmetries, respectively. All coordinates were optimized for each structure with $q = +1, 0, −1$, maintaining the geometrical restrictions of symmetry. The multiplicity for all geometries studied was 4, 5, and 6 for the systems with

charges +1, 0, and −1, respectively.

The resulting interaction energies (IE; IE = $E([Fe–CH_4]^q) − E([Fe]^q) − E([CH_4])$, where $E([A])$ is the total energy for the system A), electronic configurations (EC) of the iron atom, charges on the Fe, C, and H¹ atoms, equilibrium bond distances (EBD), Mulliken bond orders (MBO), and diatomic energies (DE) for Fe–H¹, Fe–C, C–H¹ and C–H², are presented in Tables I–III for the neutral, positive, and negative Fe–CH₄ systems, respectively. The geometry given in Figure 1a was not included because the interaction between the methane molecule and the iron atom is repulsive in all cases. This feature may be explained in terms of orbital symmetry, i.e., there are not the metallic orbitals with the required symmetry to transfer electronic density from the metal to σ* methane orbital or from the methane σ orbital to the metal, as has been proposed in other calculations.[9,13d,e]

I. [Fe–CH₄]⁰ Systems. The interaction of the methane molecule with Fe⁰ leads to thermodynamically unstable species (i.e., IE > 0), with respect to Fe[4s²3d⁶] plus CH₄, regardless of the symmetry studied. These results are in agreement with the cryogenic matrix observations obtained by Ozin et al.[13d] and Barrett et al.[13p] where binding interactions between methane and iron in its ground-state configuration were not found. If the reference state Fe*(4s¹3d⁷) is considered (the Fe*(4s¹3d⁷) is experimentally about 20 kcal/mol higher in energy than the Fe(4s²3d⁶)[25]), the Fe–CH₄ system would be slightly stable (−8.4, −3.4, and

(23) Blyholder, G.; Head, J.; Ruette, F. *Surf. Sci.* **1983**, *131*, 403.
(24) (a) Blyholder, G.; Zhao, K.-M.; Lawless, M. *Organometallics* **1985**, *4*, 1371. (b) Blyholder, G.; Lawless, M. *J. Am. Chem. Soc.* **1989**, *111*, 1275.

(25) McKee, M. L. *J. Am. Chem. Soc.* **1990**, *112*, 2601.
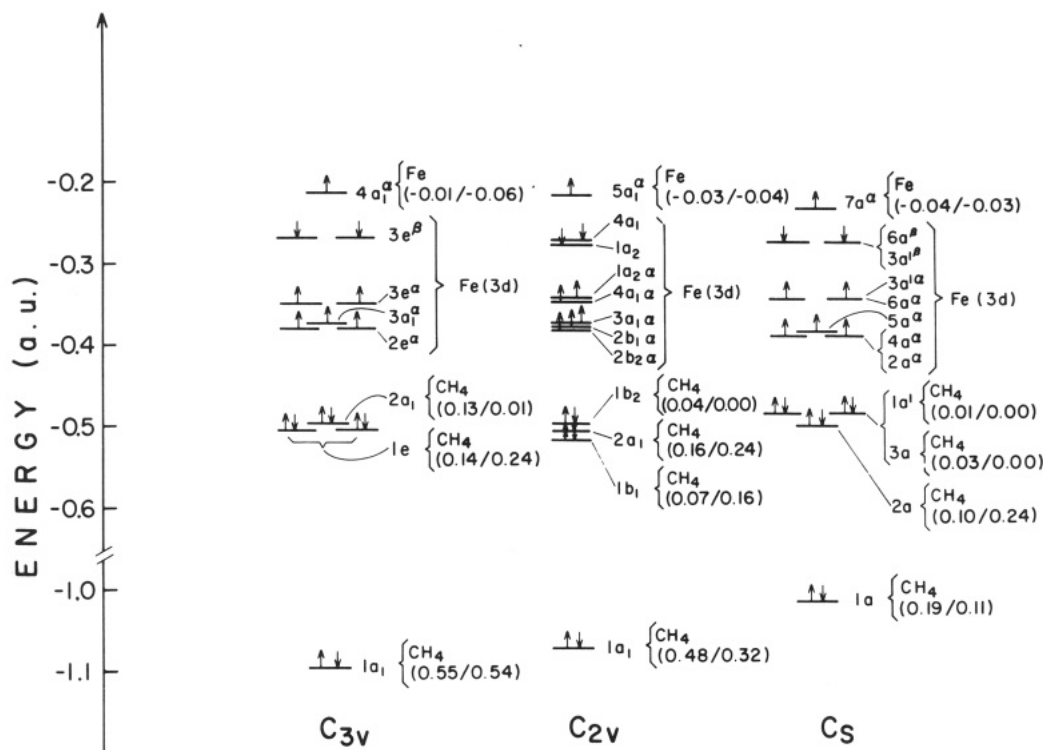
Figure 2. Energy level diagrams for the FeCH$_4$ intermediates with C_{3v}, C_{2v}, and C_s symmetries. Values in parentheses are bond-order contributions for Fe–C and Fe–H^1 bonds (MBO(Fe–C)/$\sum_i$(MBO(Fe–H^1_i))).

−5.5 kcal/mol for C_{3v}, C_{2v}, and C_s symmetries, respectively). Because it is well-known that an electronic promotion from s^2d^6 to s^1d^7 (refs 26 and 27) is required to bind Fe with a ligand, and from previous calculations with iron clusters[24] it is known that the EC of active sites resulted in mostly $(sp)^1d^7$, in this work, the excited configuration Fe*-$(4s^13d^7)$ is used for neutral systems.

The following features arise from the analysis of Table I:

(a) The EBDs, MBOs, and DEs indicate that in the Fe*CH$_4$ intermediate there is a bonding interaction mainly between Fe* and C atoms.

(b) There is electronic density transfer from methane to iron occurs, which is localized on the Fe(4p) orbitals, as is shown in the EC(4p) populations (0.41, 0.38, and 0.14 for C_{3v}, C_{2v} and C_s symmetries, respectively).

(c) An activation of the C–H bonds is observed. A comparison of the EBDs, MBOs, and Des for C–H bonds in FeCH$_4$ with those of the free CH$_4$ molecule (EBD = 1.101 Å, MBO = 1.25, and DE = −0.447 au) confirm it. As it is expected, the hydrogens (H^1) that directly interact with the iron atom are more activated than those that are far away (H^2).

(d) The relative stability of the FeCH$_4$ intermediates does not follow a consistent pattern. According to the IEs, the order must be $C_{3v} > C_s > C_{2v}$, the energy differences being very small. Nevertheless, by analyzing the BEs and DEs, the order of stability clearly is $C_{3v} > C_{2v} > C_s$.

To qualitatively understand the interaction between methane and iron centers, we present in Figure 2 the MO diagrams of Fe–CH$_4$ for the C_{3v}, C_{2v}, and C_s geometries. Each molecular orbital is characterized according with the contribution coming from the Fe or the CH$_4$ fragment. In addition, the partitioned Mulliken bond order for the Fe–C and the sum of Fe–H^1 bonds are included in parentheses
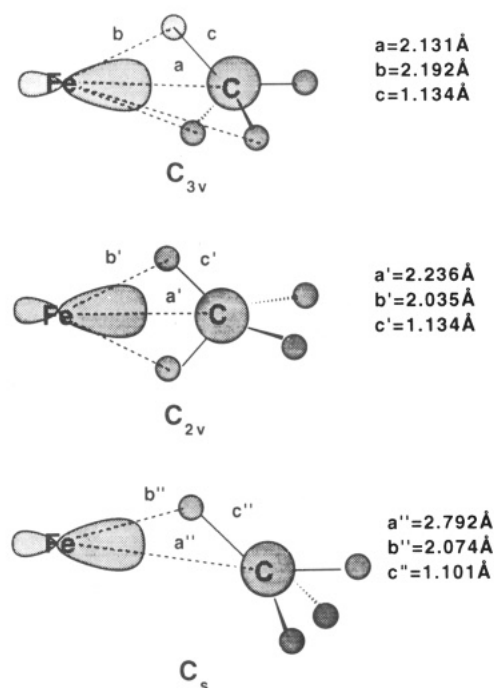
(26) Tolbert, M. A.; Beauchamp, J. L. *J. Phys. Chem.* **1986**, *90*, 5015.
(27) Blomberg, M. R. A.; Siegbahn, P. E. M.; Nagashima, U.; Wennerberg, J. *J. Am. Chem. Soc.* **1991**, *113*, 424.

Figure 3. Orbital interaction between an Fe site and the CH$_4$ molecule in different geometries: C_{3v}, C_{2v}, and C_s symmetries.

beside of each level. The most stable α and β energy levels are quasi-degenerated and therefore are represented by an average value in order to simplify the diagrams. In all diagrams the four lowest energy orbitals are mainly localized on methane while the other eight of higher energy are located on the iron atom. At first sight, it is easy to see that the lowest MOs (LMO) display the highest bond interaction, whereas the HOMO is antibonding. The mixing between Fe and CH$_4$ orbitals and the stability of the LMO augment in the order $C_{3v} > C_{2v} > C_s$, which may explain the relative stability of these three geometries. This fact can also be accounted for in the number of

overlappings between the C–H(σ) orbitals and the Fe ones: three for the C_{3v}, two in the C_{2v}, and one to the C_s symmetries, respectively, shown in Figure 3. In addition, results for the Fe–C diatomic energies and interaction energy also show the same order in stability, as can be seen in Table I. The charge transfer from CH_4 to Fe can be inferred from these diagrams because the strongest interactions resulted to be between the totally occupied orbitals on methane and the empty orbitals on Fe.

The comparison of these results with those presented by Anderson and Baldwin,[28] for the same system, shows some differences and similarities: the iron–methane interactions calculated by ASED-MO theory are weak, as is found in this work. Nevertheless, the geometry 1a, shown in Figure 1, is stable contrary to the results obtained in these calculations. Furthermore, the Fe–C distances obtained by these researchers (3.4 Å) are larger than those found in this work (2.1 Å).

Ab initio calculations carried out by Blomberg et al.[27] for the $FeCH_4(C_s)$ system at CI level show different results. The existence of an intermediate $FeCH_4$ is not reported. This may be explained by the fact that the chosen reference state in Blomberg et al.'s calculations was a low-spin $^3F(3d^74s^1)$ state.

Other calculations with similar systems have been performed by Ozin et al.[13d] employing open-shell restricted Hartree–Fock formalism and using the ^2P state of Li as a model for the related ^2P state of Cu. They found that the geometry 1a (see Figure 1) is unstable and leads, as well as in this work, to two separated systems: CH_4 plus metal.

Experimental X-ray results for $HFe_4(\eta^2\text{-CH})(CO)_{12}$[29a] and $Fe_3(\eta\text{-H})_3(CO)_9(\mu_3\text{-CCH}_3)$[29b] complexes indicate that the Fe–CR (R = H, CH_3) equilibrium bond distances are in the range 1.826–1.948 Å. The theoretical values (2.131–2.792 Å) are larger than the experimental ones. However, these calculated values are close to experimental Fe–C distances found in some agostic systems (2.101 and 2.384 Å[13m,n]).

II. $[Fe–CH_4]^+$ Systems. In the case of a positively charged iron, the methane molecule interacts with a $Fe(d^7)$ configuration, used as reference state in the calculation of IEs. The following trends come from the analysis of Table II:

(a) There is a stronger stabilizing bonding interaction than in the neutral case. This is reflected in shorter Fe–C and Fe–H^1 EBDs, and larger absolute values of the corresponding MBOs, DEs, and IEs, for all geometries. These theoretical results, as well as previous ones,[30] suggest that $[FeCH_4]^+$ complexes may exist. Methane–metal complex formation is experimentally supported by the reported $[CH_4\text{-Mn}(CO)_5]^+$ complex[31a] obtained from methane interaction with a positively charged $[Mn(CO)_5]^+$ organometallic fragment, the CH_4FeO^+ intermediate,[31b] and evidence given by Larsen and Ridge[31c] for the existence of a loosely bound complex $FeCH_4^+$.

(b) A major electronic charge transfer from CH_4 to the Fe(4s) and Fe(4p) orbitals is observed as a consequence of the positive charge on the active site.

(c) The stability of the $[Fe–CH_4]^+$ complexes is in the order $C_{3v} \sim C_{2v} > C_s$. The binding interaction is mainly through the Fe–C bond, except for the C_s symmetry, where the MBOs and DEs indicate equivalent Fe–H^1 and Fe–C interactions.

(d) The activation of the C–H^1 bonds is higher in the positively charged systems than in the neutral ones. This is shown in the comparison of the DEs (–0.394, –0.383, and –0.408 au) of neutral case with those (–0.367, –0.347, –0.341 au) of the positively charged, for C_{3v}, C_{2v}, and C_s, respectively. A similar trend is found for the MBOs, which is also reflected in an enlargement of the C–H^1 distances.

III. $[Fe–CH_4]^-$ Systems. The increase of the electron density on the iron center (the Fe^- reference state was $d^7s^1p^1$) produces (see Table III) the following features:

(a) There is a stronger stabilization of C_{3v}, C_{2v}, and C_s structures with respect to the other cases (see IE values). This stabilization is mainly due to a more powerful interaction between the iron atom and the carbon of methane; see values of MBO, DE, and EBD.

(b) The activation of C–H^1 bonds is noticeable. The comparison of EBD, MBO, and DE for C–H (EBD = 1.314 Å, MBO = 0.59, DE = –0.209 au for $FeCH_4(C_{2v})$) with those of methane (EBD = 1.101 Å, MBO = 1.25, and DE = –0.447 au) is a clear indication of this activation. In addition, a fair activation is observed for the C–H^2, particularly for the C_{2v} and C_s structures.

(c) The fact that the Fe atoms in the C_{3v}, C_{2v}, and C_s geometries present negative charges of –0.56, –0.42, and –0.23, respectively, indicates that a major electronic charge transfer to the methane occurs, as is expected.

(d) The stability order of the $FeCH_4^-$ intermediates with $C_{3v} > C_{2v} > C_s$. A stronger Fe–C interaction than in the anterior cases is also observed.

(e) Iron atoms, in C_{3v}, C_{2v}, and C_s geometries, present different electronic configurations that can be considered as approximately $d^7s^1p^1$, d^7p^1, and d^7s^1, respectively.

(f) The Fe–C bond distances for C_{2v} and C_{3v} symmetries (1.806 and 1.941 Å, respectively) are shorter than in neutral and positive cases, and relatively close to experimental values for iron complexes (1.826–1.948 Å).[29]

IV. Comparison between $[FeCH_4]^q$ Systems ($q = -1$, 0, +1). General features can be obtained by comparison of the properties between the different systems, shown in Tables I–III:

(a) There is a correlation between the p population and the C–H activation, i.e., as the electronic population on the p orbitals increases, the values of DE(C–^{1}H) and MBO are larger. This fact agrees with the experimental results obtained by Ozin et al.[13d] and Kakafi and Margrave et al.[13b] using cryogenic matrix techniques with Fe + CH_4. They found that an electronic promotion toward p orbitals of the iron atom is necessary in order to accomplish the activation of methane.

(b) These calculations show that the strongest binding interaction between an iron center (Fe^q) and a methane molecule occurs for q values of +1 and –1. Therefore, it is expected that the formation of organometallic complexes by the reaction of methane with positively or negatively Fe charged active sites is favored. Experimentalists have recently corroborated this hypothesis with the synthesis of $[Mn(CO)_5(CH_4)]^+$[31a] and $[(OC)_2Fe(CH_4)]^-$[32] complexes. These findings are consistent with the theoretical trends, because in these complexes the formal charge is located on the metals and it is expected that naked metal atoms must be more reactive than those surrounded by ligands.

(28) Anderson, A. B.; Baldwin, S. *Organometallics* **1987**, *6*, 1621.

(29) (a) Beno, M. A.; Williams, J. M.; Tachikawa, M.; Muetterties, E. L. *J. Am. Chem. Soc.* **1981**, *103*, 1485. (b) Wong, K. S.; Haller, K. J.; Dutta, T. K.; Chipman, D. M.; Fehlner, T. P. *J. Am. Chem. Soc.* **1982**, *21*, 3197.

(30) Rincón, L.; Rodríguez-Arias, E. N.; Ruette, F. Proc. XII Simposio Iberoamericano de Catálisis, Instituto Brasileiro de Petróleo, Rio de Janeiro, Brasil, 1990; Vol. 3, p 308.

(31) (a) Hop, C. E. C. A.; McMahon, T. B. *J. Am. Chem. Soc.* **1991**, *113*, 355. (b) Schwarz, H. *Angew. Chem., Int. Ed. Engl.* **1991**, *30*, 820. (c) Larsen, B. S.; Ridge, D. P. *J. Am. Chem. Soc.* **1984**, *106*, 1912.

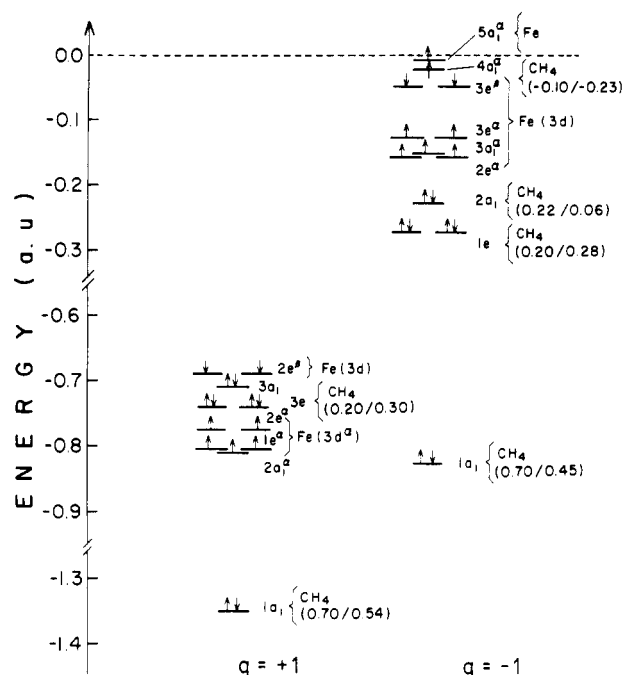(32) McDonald, R. N.; Jones, M. T.; Chowdhury, A. K. *J. Am. Chem. Soc.* **1991**, *113*, 476.

Figure 4. Energy level diagrams for the $[FeCH_4]^q$ intermediates (q = +1, -1) with C_{3v} symmetry. Values in parentheses are bond-order contributions for Fe–C and Fe–H^1 bonds (MBO(Fe–C))/$\sum_i$(MBO(Fe–H^1_i)).

Figure 5. Potential energy curves for dissociation of C–H bond in $[FeCH_4]^q$ complexes (q = +1, 0, -1) with C_s symmetry.

(c) From an analysis of the diatomic energies (DE(Fe–C) and DE(C–H^1)), it can be seen that a negative charge noticeably favors the formation of $FeCH_4^-$ complexes and the activation of C–H bonds for each of the geometries studied. The C_{2v} configuration being the most favored. A Fe–C strong bond is formed with a partial formation of Fe–H^1 bonds. Relatively short Fe–C bond distance (1.806 Å) is found and electronic charge transference from the iron to the H^1 atom occurs, which is characteristic of metal hydrides. Furthermore, it can be observed that C–H^1 bond orders and their diatomic energies become smaller than in the case of free CH_4. A similar effect, but of minor magnitude, is observed in the positively charged systems.

With the purpose of explaining the trends of methane interaction, as the charge of the active site changes, the molecular orbital diagrams for $[FeCH_4]^q$ (q = -1, +1) systems with C_{3v} symmetry (see Figure 1b) are presented in Figure 4. The MO are similar to those shown in Figure 2, for the neutral systems. The differences with the previous ones are in the eigenvalue energies and in the orbital mixing. The negative charged system shows eigenvalues at higher energies (i.e., less stable than the neutral system (see Figure 2)), whereas the positively charged one lies at lower energies (more stable). If the magnitude of the bond orders are compared, it is clear that the amount of mixing among the orbitals is in the order $[FeCH_4]^-$ > $[FeCH_4]^+$ > $[FeCH_4]^0$. In the case of the negatively charged system, the occupied Fe(4p) orbital can strongly interact with the antibonding C–H orbital on methane, which causes the activation on the C–H bonds, because of the donation from metal to methane. In the case of $[FeCH_4]^+$, the total bonding interaction, with respect to the neutral system, increases because the antibonding interaction that appears in $[FeCH_4]^0$ disappears, as the HOMO orbital is emptied. Thus, these molecular diagrams may explain the augment of Fe–CH_4 interaction energy in the order Fe^- > Fe^+ > Fe^0 and the higher activation of methane observed in the negative system.

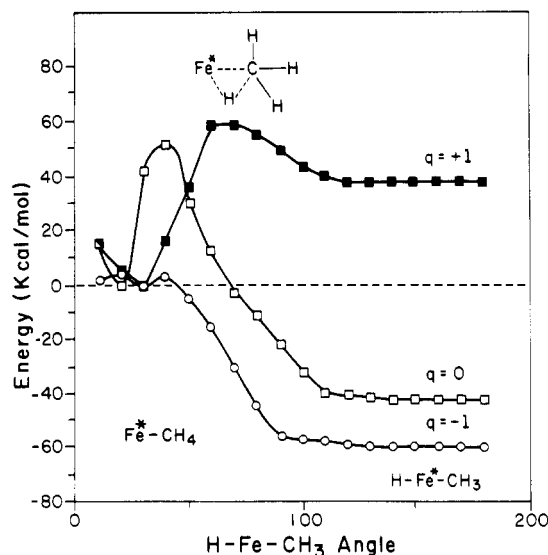One can conclude from this section that the main factor that governs the formation of $[FeCH_4]^q$ intermediates is

the transfer of electronic density from the metal toward the ligands and vice versa. In the case of Fe^+ the electronic drift from methane stabilizes the $[Fe^+ + CH_4]$ system, whereas in the case of Fe^- the excess of electronic density is smeared out into the methane molecule.

C–H Bond Dissociation

To study the C–H bond oxidative addition process, the C_s symmetry system was chosen, among all geometries studied, because it presents the largest Fe–H interaction and the correct symmetry for breaking one C–H bond. Potential energy curves along the C–H dissociation path was calculated by changing the C–Fe–H^1 angle, as shown in Figure 5. All coordinates were optimized for each C–Fe–H^1 angle, and the $[FeCH_4]^q$ complexes were taken as reference for zero energy.

The results reveal that the positively charged and neutral systems present a high activation barrier (50–60 kcal/mol) for the C–H bond dissociation process. It can be also noted that in the positively charged case this process is thermodynamically disfavored. On the other hand, the C–H bond dissociation is favored in the negatively charged system.

A comparison of orbital population of iron atoms on $[FeCH_4]^q$ intermediates (Fe^0 $(s^{0.98}p^{0.14}d^{7.00})$, Fe^+ $(s^{0.14}p^{0.18}d^{7.00})$, Fe^- $(s^{0.96}p^{0.27}d^{7.00})$) and dissociated species Fe^0 $(s^{0.89}p^{0.87}d^{6.02})$, Fe^+ $(s^{0.91}p^{0.71}d^{6.03})$, Fe^- $(s^{0.51}p^{0.65}d^{6.99})$) indicates that an internal electronic transference in the metal atom toward 4p orbitals occurs. This fact, as was pointed out above, is supported by cryogenic matrix results, where the methane molecule can be dissociated in the presence of an iron atom if it is radiated with light that permits a d → p electronic transition.[13e] These results can be interpreted on the basis of the electronic correlation diagram analysis between intermediate and dissociated species; see Figure 6.

The electronic correlation diagram for α electronic spins, Figure 6a, shows that all d orbitals of the metal atom are stabilized as methane dissociates, whereas some methane orbitals are slightly destabilized. The LUMO orbital (8a) is formed by CH_4 antibonding orbitals with a small contribution of the Fe($4p_z$) orbital, and it is stabilized as the reaction coordinate increases. If the system is negatively charged with high spin, this orbital in $[FeCH_4]^-$ is occupied and 0.77 electron is transferred to the methane (see Table III), resulting in a substantial weakening of the C–H bond
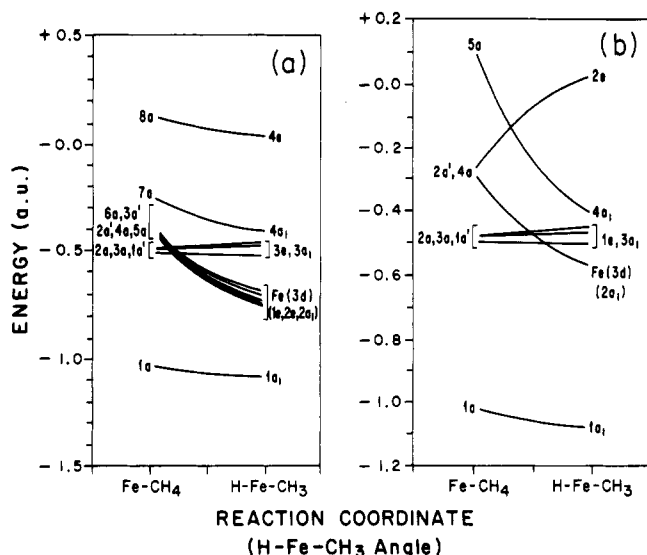
Figure 6. Correlation diagrams for C–H dissociation of CH_4 on an Fe atom: (a) for α electrons; (b) for β electrons.

and a stabilization of the system. In the case of β-spin orbitals, shown in Figure 6b, the HOMO orbital, essentially formed by a $3d_{z^2}$ (4a) orbital, is destabilized while LUMO orbital formed by a $4p_z$ (5a) is strongly stabilized. These characteristics consistently suggest that a $[CH_4Fe]^q$ intermediate would be dissociated by undergoing an d → p electronic transition.

The facility of Fe^q active sites for dissociating C–H bonds can be explained by the ECs (Fe) (Fe^+ (d^7), Fe^0 (d^7s^1), and Fe^- ($d^7s^1p^1$)). The iron state with charge –1 is adequate to dissociate the molecule and shows the lowest activation barrier in Figure 5. On the other hand, the neutral and positive complex require a d → p transition, explaining in this way the high activation barriers appearing in Figure 5.

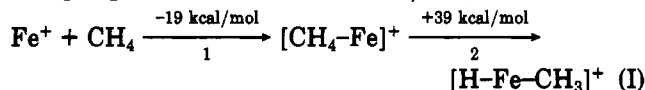The observed trends for Fe^q charged systems, see Figures 5 and 6, are similar to those obtained for $Fe^q + H_2$ ($q = 1, 0, -1$),[15] where a detailed search of different electronic states were performed.

Comparison with Experimental Results. These calculations show that the Fe + CH_4 interaction is exothermic, contrary to experimental findings. Nevertheless, it is necessary to consider that our reference state (s^1d^7) is experimentally 20 kcal/mol higher in energy than the ground state. In addition, the parameters employed here seem to overestimate the C–Fe interaction. However, methane activation has recently been achieved by using intermediate unsaturated species, photochemically generated ($Fe(L)_2$ ($L = R_2PCH_2CH_2PR_2$, $R = Me$, Et)).[13q]

Experimental results of ion beam studies with methane and metal cations of group 8 (Fe, Co, Ni)[33] reveal that the reaction

$$Fe^+ + CH_4 \rightarrow [H-Fe-CH_3]^+$$
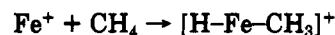
is an endothermic process with a heat of reaction of 22 kcal/mol. The energy sum of the processes 1 and 2, shown in eq I, gives the value of 20 kcal/mol, in remarkable

$$Fe^+ + CH_4 \xrightarrow[\quad 1 \quad]{-19 \text{ kcal/mol}} [CH_4-Fe]^+ \xrightarrow[\quad 2 \quad]{+39 \text{ kcal/mol}}$$
$$[H-Fe-CH_3]^+ \quad \text{(I)}$$

agreement with the experimental findings. It is good to note that the reference state ($^4F(d^7)$) is an excited state, with 5.3 kcal/mol higher in energy than the ground state ($^6D(d^6s^1)$).

In the case of $Fe^-(d^6sp) + CH_4$, the exothermicity is supported by experiments performed by Ozin et al.[13e,d] with $Fe(d^6sp)$ at very low temperature in cryogenic matrices. The oxidative addition of methane occurs with a very low activation barrier, going from high-energy reactants ($Fe^* + CH_4$) and the intermediate (HFe^*CH_3) to a low-energy final product ($H-Fe-CH_3$). The oxidative insertion into the C–H bond by the $[(OC)_2-Fe]^-$ complex, reported by McDonald et al.[32] to form the $[(OC)_2-Fe(H)(CH_3)]^-$ adduct, can also be taken as an indication of the higher reactivity of the Fe^- center with respect to the Fe^0 one.

Conclusions

These qualitative calculations of Fe–CH_4 interaction and oxidative addition of methane on modeled iron metal centers Fe^q ($q = +1, 0, -1$) reveal the following features:

(i) The formation of methane–iron intermediates (adsorbed species) on an iron atom is feasible, especially if Fe is negatively or positively charged. The stabilizing interaction is primordially between carbon and iron atoms.

(ii) A d → p electronic transition favors the formation of these $FeCH_4$ intermediates as well as oxidative addition of methane.

(iii) The C–H bond dissociation is considerably favored when the active site has extra electronic density available (Fe^-) that can be transferred to the methane.

(iv) MINDO/SR calculations carried out at a very qualitative level (without searching for stability of different electronic states and very simple parametrization) can give valuable information that it is supported by experimental results.

(33) Halle, L. F.; Armentrout, P. B.; Beauchamp, J. L. *Organometallics* **1982**, *1*, 963.